DISCOVERIE

Project No. 848228

DISCOvERIE

Development, dIagnostic and prevention of gender-related Somatic and mental COmorbitiEs in iRritable bowel syndrome In Europe

Workpackage 4
Deliverable D4.2
Profiling of “gut-to- brain” and “brain- to-gut” mechanisms associated with comorbidities development in IBS

Start date of project: 2020-01-01

End Date: 2024-12-31

Duration: 60 months

Organisation name of lead contractor for this deliverable:

Partner 6: Katholieke Univeriteit Leuven, KUL

Project co-funded by the European Commission within the Horizon 2020 research and innovation programme under Grant Agreement No 848228		
Dissemination Level		
PU	Public	X
PP	Restricted to other programme participants (including the Commission Services)	
RE	Restricted to a group specified by the consortium (including the Commission Services)	

CO	Confidential, only for members of the consortium (including the Commission Services)	

Disclaimer

This document is an output of a project grant (Grant Agreement nº: 848228) funded under H2020 Research Programme of the European Commission. The content of this document represents the views of the author only and is his/her sole responsibility; it cannot be considered to reflect the views of the European Commission or any other body of the European Union. The European Commission do not accept any responsibility for use that may be made of the information it contains.

Consortium

Partcicipant Nº	Participant Legal Name	Country	Partner's Acronym
1	Fundacio Hospital Universitari Vall d'Hebron-Institut de recerca	ES	VHIR
2	Goeteborgs Universitet	SE	UGOT
4	University College Cork – National University of Ireland, Cork	IE	UCC
5	Johann Wolfgang Goethe – Universitatfrankfurt Am Main	DE	GUF
6	Katholieke Univeriteit Leuven	BE	KUL
7	Universitatsklinikum Heidelberg	DE	UKL-HD
8	Alma Mater Studiorum – Universita Di Bologna	IT	UNIBO
9	VIB VZW	BE	VIB
10	Universiteit Maastricht	NL	UM
11	Semmelweis Eguetem	HU	SU
12	Universitatea de Medicina Si Farmacie Iuliu	ROU	UMF
13	Anaxomics Biotech, S.L.	ES	AX
14	Hycult Biotechnology BV	NL	HB
15	Emergentec Biodevelopment GMBH	AU	EMTEC
16	Nanostring Technologies Inc	USA	NSTG
17	Cliclab Technologies Inc	ES	Cliclab
18	Followhealth SL	ES	hITc
19	BYTE Factory Systems SL	ES	BF
20	Stichting Radboud Universitair Medisch Centrum	NL	RUMC

Table of Contents

Table of Figures

List of Abbreviations

BBB: Blood-brain barrier

BBDP: Bio-breeding diabetes-prone

ce-MRI: Contrast-enhanced magnetic resonance imaging

CFS: Chronic Fatigue Syndrome

DGBI: Disorder of gut-brain interaction

EMP: Elevated Plus Maze

HPA Axis: Hypothalamic-Pituitary-Adrenal axis

IBS: Irritable Bowel Syndrome

MRS: Magnetic Resonance Spectroscopy

TEER: Transepithelial electrical resistance

TFT: Tail Flick Test

WP: Work Package

Executive summary

Background: Irritable bowel syndrome (IBS) is defined as a disorder of gut-brain interaction. Several alterations at the brain and intestinal level have been described in IBS patients. Nevertheless, the exact sequence of events is unknown. Moreover, whether alterations in the gut can induce somatic and psychological comorbidities is a matter of discussion.

Aim: This report aims to present the work done in the context of *Work Package 4 "Central Nervous System and Stress Axis Function", task T4.4) Unravelling gut-to-brain and brain-to-gut signaling mechanisms underlying mental and somatic comorbidity development in rodents* as per Grant Agreement. We aimed to determine whether alterations in the gut, such as increased intestinal permeability, can affect brain function and consequently explain the comorbidities commonly present in IBS patients.

Methods: To tackle this complex objective, we employed a comprehensive approach. Different animal models were used in the context of the DISCOvERIE project at KUL and UCC centers. In this D4.2 report, we had focused only on one of the rat models, namely the bio-breeding diabetes-prone (BBDP) model. We meticulously assessed the paracellular and transcellular small intestinal and colonic permeabilities in vivo by gavaging FD4 and TRICT70, the blood-brain barrier (BBB) permeability using contrast-enhanced magnetic resonance imaging, brain metabolites using proton magnetic resonance spectroscopy, anxiety-like behaviour with the elevated plus maze and somatic pain using the tail-flick test.

Results: BBDP rats develop an increased colonic transcellular permeability at an early age. Interestingly, this increased permeability is succeeded by, and associated with, increased BBB permeability in late adulthood only in the anterior cingulate cortex but not in the insula and the hippocampus. Surprisingly, BBDP rats also showed alterations in brain metabolite profile, independently of intestinal and BBB permeability. BBDP rats did not show signs of brain neuroinflammation either in the ACC or insula. Moreover, BBDP rats develop higher levels of somatic pain at an early age and anxiety-like behaviour in late adulthood.

Conclusion: Results from the BBDP rat model do not support the underlying premise of the DISCOvERIE project and the current hypothesis that an increased gut permeability leads to brain neuroinflammation and, consequently, psychological (anxiety) and somatic

comorbidities. A second version of this deliverable will be submitted by the end of the year 2024 in order to include also the analyses of the other two rat models (faecal microbiota transplantation and early life stress), providing us with further insights into the IBS pathogenesis and the associated comorbidities.

Introduction

Irritable bowel syndrome (IBS) is a common disorder of gut-brain interaction (DGBI) defined by abdominal pain accompanied by altered stool patterns in terms of frequency and consistency[1], with an estimated prevalence of 4%[2]. IBS has a significant personal, societal, and economic disease burden. This burden is magnified by the widespread presence of comorbidities, including mental comorbidities (such as anxiety, depression) and functional somatic comorbidities such as fibromyalgia (widespread chronic pain) and chronic fatigue syndrome (CFS)[3,4].

IBS is classified as a disorder of gut-brain interaction. While the exact cause of IBS is still unknown, many mechanisms along the entire microbiota-gut-brain axis have been implicated in IBS. On the “brain” side of the gut-brain axis, stress and the activation of the HPA axis have been implicated. On the intestinal level, low-grade inflammation and increased intestinal permeability have been suggested to play an essential role in the IBS pathophysiology. The current hypothesis, but not supported scientifically, is that altered permeability and low-grade inflammation increase the blood-brain barrier permeability, inducing brain neuroinflammation. These brain abnormalities alter brain function and lead to mental and somatic comorbidities.

Some but not all of these alterations have also been described in IBS patients, but the exact sequence has yet to be discovered. Therefore, the overall goal of D4.2 is to identify the temporal/causal order of gut-to-brain and brain-to-gut signalling mechanisms underlying comorbidity development in rodent models. For this purpose, we will use three different animal models: 1) the bio-breeding diabetes-prone (BBDP) rat and the faecal microbiota transplantation models to better understand the gut-brain interactions, and 2) the maternal separation rat model to disentangle the brain-gut interactions. In the current version of the D4.2, it is included only the BBDP rat model.

Detailed description of the methods used & the work performed

T4.4: Unraveling gut-to-brain and brain-to-gut signalling mechanisms underlying mental and somatic comorbidity development in rodents

Methods – Animals

The BioBreeding diabetes-prone (BBDP) and control BioBreeding diabetes-resistant (BBDR) rats were purchased from the Animal Resources Division of Health Canada, Ottawa, ON, Canada, and further bred in the animal facility at KU Leuven. Rats were housed in open cages, at ambient temperatures (22±2°C), with 14 hours light per day (7h – 21h) and were given regular rat chow food and water *ad libitum*. Glycaemia levels of BBDP rats were checked each week on tail blood using a OneTouch®Verio® glucometer (LifeScan) starting from 60 days of age. Onset of diabetes was considered if the threshold of 250 mg/dL was reached on two consecutive measurements. Diabetic animals were subcutaneously implanted with sustained release insulin implants (LinShin Canada, Inc.) Animals selected to undergo experiments at 30, 90, 160 and 220 days of age were moved to the experimental facility and kept in individually ventilated cages (IVC). 16 BBDP (9 males and 7 females) and 17 BBDR (10 males and 7 females) rats started the experiments; however, some experiments had to be excluded due to technical problems and drop out of sick rats.

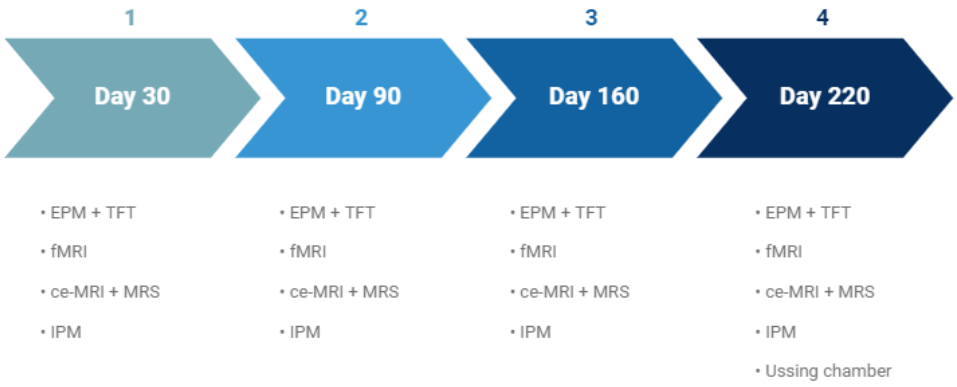

Figure 1 - Behavioural, somatic and intestinal experiments on animals
Animals underwent a series of behavioural (elevated plus maze, EPM), somatic (tail flick test, TFT), brain (functional MRI, contrast enhanced MRI and MRS) and intestinal (intestinal permeability and motility, IPM) experiments at four timepoints, when the rats were 30, 90, 160 and 220 days old. After the last timepoint, rats were sacrificed to assess intestinal permeability ex vivo using Ussing chambers.

An additional study was performed on Sprague-Dawley rats to study the role of the microbiome on the development of IBS and psychological comorbidities. Rats underwent an antibiotic cocktail therapy for one week to deplete the intestinal microbiome, after which human faecal samples from IBS patients, with and without mental comorbidities, were administered via oral gavage. The rats then underwent the same experiments as those of the BBDP study. However, this version of the deliverable focuses only on the BBDP study.

Intestinal permeability and motility *in vivo*

Intestinal permeability was assessed in vivo by measuring the passage of fluorescently labelled dextrans from the GI tract to the blood[5]. A smaller molecule (4 kDa) is used to assess the paracellular route, whereas a larger molecule (70 kDa) reflects the transcellular route[6].

Rats were fasted for two hours except for access to water. Rats were then anaesthetised with 3.5% isoflurane (Iso-vet, 1000 mg/g, Piramal Critical Care, Netherlands) after which a baseline blood sample (± 200 µL) was taken via saphenous vein puncture. Then a solution of 30 mg/ml of fluorescein isothiocyanate 4-kDa Dextran (FD4) and Tetramethylrhodamine isothiocyanate–Dextran (TRITC-70) 70 kDa (TdB Labs, Sweden) dissolved in PBS was administered (0,5ml/100g rat) via oral gavage, after which food was newly provided to the rats. After 3 h, and 24 h, another blood sample was taken. Meanwhile, faecal pellets were visually checked for redness, to assess the motility via the transit time of TRITC-70, which colours the faeces brightly red, with a cut-off time of 10 hours. Blood samples were immediately placed on ice and centrifuged. Plasma concentration of FD4 and TRITC-70 was determined by measuring the fluorescence intensity of FD4 (485 nm/520 nm) and TRITC-70 (544 nm/590 nm) using a spectrophotometer (FluoSTAR Omega, BMG Labtech).

Intestinal permeability ex vivo assessed with the Ussing chamber technique

Intestinal permeability was assessed ex vivo using Ussing chambers [7](111). The Ussing chamber consists of two half-chambers, between which the intestinal tissue is placed (112). A physiological solution (i.e. Kreb's Ringer solution) is

added to the serosal and mucosal sides to maintain tissue viability, and electrodes are used to measure the ion transport[8] (112).

Krebs buffer was prepared dissolving 118.04 mM KCl, 24 mM $MgCl_2$ x $6H_2O$, 24 mM NaH_2PO4 x H_2O, 22.58 mM $CaCl_2$ x $2H_2O$,glutamate (6.5 mM), pyruvate (7.15 mM), NaCl (120.8 mM) and $NaHCO_3$ (14.28 mM) in milliQ water. For the luminal side, mannitol (11.42 mM) was added, whereas for the basolateral side glucose (11.55 mM) was added. Solutions were brought to pH 7.2 with 1M HCl, oxygenated with carbogen (95% O2, 5% CO2) and kept at 37°C for the duration of the experiment. FD-4 and TRITC-70 (Tdb Labs, Sweden), were dissolved in Mannitol-Krebs.

Rats were sacrificed via decapitation and the large intestine was collected in Glucose-Krebs and kept on ice. Three segments of distal colon of approximately 1 cm were mounted on the Ussing chamber (Mussler Scientific Instruments, Aachen, Germany), exposing 0.096 cm2 of intestinal tissue to Mannitol-Krebs on the luminal side and Glucose-Krebs on the basolateral side. The Ussing chambers were oxygenated with carbogen (95% O2 and 5% CO2) and kept at 37°C. After a 20-minute equilibration period, a baseline sample was taken from the basolateral side, after which 30 µL of FD-4 and TRITC-70 were added to the luminal side, resulting in a concentration of 1 mg/mL.

Ussing chambers were connected to a voltmeter to measure the transepithelial electrical resistance (TEER) and potential differences (using Ag/AgCl electrodes), as a measure of ion flux and barrier function. Samples were taken from the basolateral side after 60 min, 90 min and 120 min.

Passage of FD4 and TRICT-70 is determined by measuring the fluorescence intensity respectively at 493 nm/518 nm and at 550 nm/571 nm using a spectrophotometer (FluoSTAR Omega, BMG Labtech).

Assessment of somatic pain: the tail flick test

The tail flick test (TFT) is used for the measurement of nociception in rodents. Usually, a heat stimulus is applied to the tail, and the latency time until the tail is rapidly removed from the water, a tail-flick, is measured[9].

Rats were assessed for somatic pain using the TFT. Rats were restrained with a fabric restrainer, and approximately half of the tail was submerged in hot water (55°C). The tail-flick latency was measured using a stopwatch, with a cutoff time of 5 seconds to avoid burning damage. The test was repeated three times, and the average latency time was calculated.

Behavioural assessment of anxiety: the Elevated Plus Maze

The elevated plus maze (EPM) is a validated method for the measurement of anxiety levels in rodents[10]. It assesses the approach-avoidant behaviour of rodents, where rats will naturally prefer the dark spaces of the closed arms, and avoid the open, illuminated arms[11].

The EPM consisted of four black polypropylene arms cross-shaped towards a central platform (10 cm x 10 cm), all elevated 50 cm above the floor. The two open arms (50 cm long, 10 cm wide) and two closed arms (50 cm long, 10 cm wide, with 40 cm high walls) were placed opposite of each other and at a 90° angle. The test occurred in a dimly lit room and rats were habituated to the room 30 minutes before the experiment. Rats were placed in the centre of the EPM, facing towards an open arm, and allowed to explore the maze for five minutes while their behaviour was recorded with a video camera connected to AnyMaze software (AnyMaze 7.2). The following behavioural parameters were assessed: number of entries in the open and the closed arms (an entry is considered when all four paws are in the designated zone) and the percentage of time spent in the closed and open arms. The EPM was cleaned with 70% EtOH between each animal.

Assessment of blood-brain-barrier integrity: contrast-enhanced magnetic resonance imaging

Contrast-enhanced magnetic resonance imaging (ce-MRI) is an MRI-technique where a paramagnetic compound, usually gadolinium-based, is injected intravenously, resulting in a shorter proton relaxation time and thus a stronger signal intensity in so-called T1-weighted MR images[12]. The blood-brain-barrier is usually impenetrable for gadolinium; however, when this barrier is disrupted, an increased passage of contrast agent will result in a stronger signal (quantified as a lower T1-value)[13]. T1-values allow a relative assessment of the contrast agent accumulation in the brain and can be determined by the acquisition of parametric T1-maps.

Rats were habituated to the MRI room for 30 minutes prior the experiment. Then they were anaesthetised with 3,5% - 4% isoflurane (Iso-vet, 1000 mg/g, Piramal Critical Care, Netherlands) in 100% oxygen, after which a catheter was placed in the tail vein and the rat was tightly secured in an open MRI rat bed in a prone posture. Once the animal was securely positioned, the isoflurane was decreased 2%. The rat bed was heated with warm water (45°C) and the body temperature and respiration rate were monitored with PC-SAM software (version 8.0.2, Small Animal Instruments, Incorporated) and maintained at physiological levels of 40-60 min-1 and 37 +/- 1℃ , respectively. A 7 Tesla MRI scanner (biospec 70/30, Bruker, Biospin, Ettlingen, Germany) was used with a BG20S imaging gradient system, an 86 mm 1H transmit quadrature volume coil (112/086 QSN TO AD volume coil, Bruker) with active detuning and a 1H receive rat brain surface coil (300 1H R BR surface coil, Bruker). The scanning sequences were executed using Paravision 6.0.1.

A T2-weighted anatomical MR image was acquired using a Turbo RARE sequence with the following parameters: TE/TR = 36/2056 ms, averages = 2, RARE factor = 8, echo spacing = 12 ms, slice orientation = axial (16 slices), slice thickness = 1 mm, field of view (FOV) = 40 x 40 mm, matrix size = 256 x 256, resolution = 0.156 x 0.156 mm.
A T1 map before and after injection of the gadolinium-based contrast agent (0.25 mL/100 g rat weight of 0.05 mM, gadoterate meglumine, DOTAREM®) was obtained using a RARE VTR (variable repetition time) sequence with the following parameters: TE = 23.17 ms, TRs = 550 ms, 800 ms, 1500 ms, 3000 ms, 6000 ms; averages = 1, RARE factor =

6, echo spacing = 7.724 ms, slice orientation = axial (8 slices), slice thickness = 1 mm, field of view (FOV) = 40 x 40 mm, matrix size = 128 x 128, resolution = 0.313 x 0.313 mm. To check whether contrast injection was successful, a dynamic contrast enhanced (DCE) FLASH (fast low angle shot) image sequence was obtained between the pre- and post-T1map acquisition with the following parameters: TE/TR = 2.896/59.3 ms, averages = 1, flip angle = 40°, slice orientation = axial (8 slices), slice thickness = 1 mm, field of view (FOV) = 40 x 40 mm, matrix size = 128 x 128, resolution = 0.313 x 0.313 mm

The total scan time for each animal was approximately 1 hour. ce-MRI data processing

T1 maps were converted to NiFti using an in-house built script in MATLAB (version R2022b). T1 maps taken before and after injection of gadolinium were co-registered using the FLIRT linear registration tool (version 6.0) of the FSL software (5.09) in Neurodebian (8.0.0). A rigid-body transformation was used with a mutual information cost function (128 histogram bins) and Nearest Neighbour interpolation was applied. The quality of the registered images was visually checked using ITK SNAP. The T1 values (ms) were calculated using an in-house built script in MATLAB (version R2022b). The average T1 values per region of interest (ROI) were further used for statistical analysis.

ROIs for a whole brain slice (Bregma: 0.48), ACC, insula and hippocampus were drawn manually in ITK SNAP (Fig.2). Location was based on the Paxinos and Watson rat brain atlas [14].

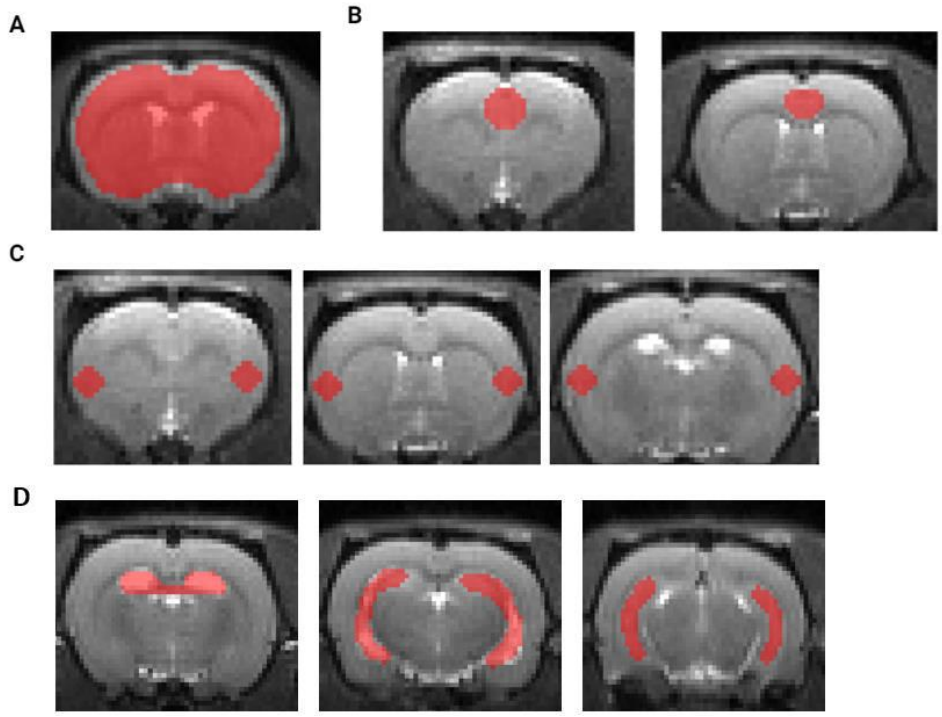

Figure 2 - Representative masks drawn manually for whole brain (A), ACC (B), insula (C) and hippocampus (D) in ITK SNAP.

Assessing the brain metabolic profile: Magnetic Resonance Spectroscopy (MRS)

Proton Magnetic Resonance Spectroscopy (^{1}H-MRS) is a non-invasive MR-technique that allows the measurement of mobile (water soluble) brain metabolites based on their hydrogen signal and unique magnetic properties[15,16]. The resonance frequency of the protons in a metabolite, which is dependent on the chemical environment, is compared to that of a reference molecule. This specific resonance frequency is called chemical shift[15]. Metabolite concentrations can be calculated by referencing signal integrals to a known reference compound, such as the unsuppressed water signal.

MRS was performed immediately after the ce-MRI. A T2-weighted anatomical image was acquired using a Turbo RARE (rapid acquisition with relaxation enhancement) sequence with the following parameters: TE/TR = 40/3000 ms, averages = 1, RARE factor = 8, echo spacing = 10 ms, slice orientation = axial (32 slices), slice thickness = 1 mm, field of view (FOV) = 35 x 35 mm, matrix size = 192 x 192, resolution = 0.182 x 0.182 mm.

A PRESS (point resolved spectroscopy) ^{1}H-MRS sequence was acquired to obtain a spectrum of the brain metabolites. The scanning sequence had the following parameters:

TE/TR = 20/2500 ms, averages = 256, flip angles of 3 RF pulses: 1: 90°, 2: 180°, 3: 180°. A voxel was placed manually over the ROI: voxel size insula: 1.5 x 1.5 x 3 mm; voxel size ACC: 1.8 x 1.8 x 3 mm. For water suppression, a VAPOR sequence was used. For later quantification, a scan without water suppression was acquired as reference.

The total scan time for each animal was approximately 30 minutes.

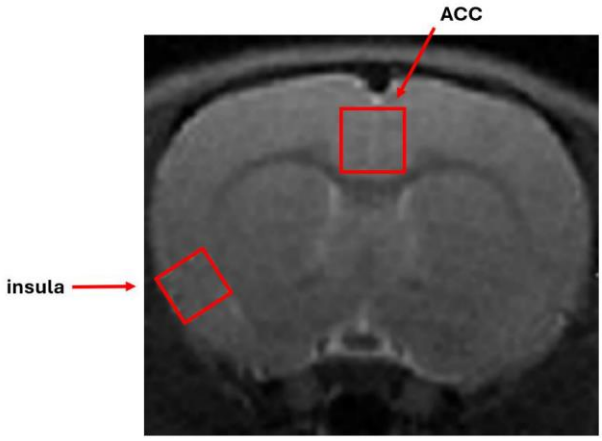

Figure 3 - Representative voxel placement of insula and ACC for MRS

MRS data processing

MRS data was analysed using LCModel (version 6.3.1R), which quantifies the metabolites by calculating the best fit of a linear combination of model spectra[17-19]. 27 metabolites were included in the basis set. Spectra were visually checked, and spectra with a signal to noise ratio < 6 for the ACC and < 3 for the insula were excluded. Metabolites with a relative CRLB (=%SD) above 20%, as calculated by LCModel were excluded. Absolute metabolite concentrations relative to the unsuppressed water resonance were used for further statistical analysis. We are particularly interested in the following metabolites myoinositol (MI), choline-containing compounds (total Choline), N-acetyl aspartate (NAA), and glutamine plus glutamate (Glx). Neuroinflammation with activated astrocytes and microglia is often associated with elevated myoinositol (MI) and, to a lesser extent, with levels of choline-containing compounds (total Choline), which are found in higher concentrations in glia than neurons. Neuronal injury is indicated by lower levels of N-acetyl aspartate (NAA) and glutamine (Glu).

Assessment of brain activity: resting-state functional MRI (rs-fMRI)

To study alterations in brain activity in the BBDP rat, rs-fMRI scans were acquired. Functional MRI is a non-invasive imaging technique that allows the measurement of brain activity based on the Blood Oxygen Dependent Level (BOLD). The BOLD effect is based on the ratio of paramagnetic deoxyhaemoglobin to diamagnetic oxyhaemoglobin, which increases after brain activation due to increased perfusion [20]. Unfortunately, due to time restrictions, the data could not be analysed yet.

Rats were habituated to the MRI room for 30 minutes prior the experiment. Then, they were anesthetized with 3.5-4% isoflurane (Iso-vet, 1000 mg/g, Piramal Critical Care, Netherlands), in a mix of oxygen (30%) and air (70%), after which they were tightly secured in an open MRI rat bed in a prone posture. To avoid confounding brain activity due to anaesthesia during the fMRI protocol, the isoflurane was lowered to 0.8-1.5% during the MRI measurements. The rat bed was heated with warm water (45°C) and the body temperature and breathing rate were monitored (with PC-SAM software (version 6.17, Small Animal Instruments, Incorporated, USA). A 9.4 Tesla MRI scanner (Biospec 94/20, Bruker Biospin, Ettlingen, Germany) was used with a BGA-12 imaging gradient system (gradient strength up to 600 mT/m, a 72 mm 1H transmit volume coil (112/072 LIN T1 0325 linear coil, Bruker) and a 1H receive rat brain surface coil (400 1 H R.BR, Bruker). The scanning sequences were executed using Paravision 360 (V3.0).

T2-weighted anatomical MR images with 20 slices in axial orientation were acquired using a Turbo RARE (rapid acquisition with relaxation enhancement) sequence with the following parameters: echo time (TE)/repetition time (TR) = 33/2500 ms, averages = 1, slice orientation = axial, slice thickness = 1 mm, image size = 256 x 256, FOV = 35 x 35 mm.

A FID-EPI (free induction decay – echo planar imaging) sequence was used to obtain T2* weighted resting-state functional images with the following parameters: TE /TR = 15.494/2000 ms, repetitions = 300, averages = 1, slice orientation = axial (20 slices, same orientation as anatomical image), slice thickness = 1 mm, field of view (FOV) = 35 x 35 mm, matrix size = 128 x 96, resolution = 0.273 x 0.365 mm.

Total scan time for each animal was approximately1 hour.

Tasks performed so far

KUL: The data collection for the BBDP rat model follow-up (30, 90, 160, 220 days) finished in June 2024. We present in the current report the data analysed at this moment. We recently started analyzing the functional MRI results, and we are including the results of the last animals, BBDP and BBDR rats. The entire results will be included in the RP4.

The faeces of all patient groups and healthy subjects were satisfactorily transplanted into the rats (the faecal microbiota transplantations model), and all the experiments were finished in June. We are currently analyzing all the data. Results will be included in the following report period.

UCC: The faeces of all groups of the patients and healthy subjects were satisfactorily transplanted to the rats, and all the experiments were finished in March. We are currently analyzing all the data. Results will be included in the following report period.

The experiments with the maternal separation model (brain-gut axis) were completely finalized in March. We are now analyzing all the data, and the results will be included in the following report period.

Statistical analysis

Statistical analyses were performed in GraphPad Prism (10.2.3). For the behavioural assessment, the number of entries and percentage of time were analysed with two-way ANOVAs (mixed effects) using the Geisser-Greenhouse correction. Post-hoc comparisons were performed by Tukey's multiple comparisons test. The average latency time of the three tail-flick measurements was analysed with two-way ANOVAs (mixed effects) using the Geisser-Greenhouse correction. Post-hoc comparisons were performed by Tukey's multiple comparisons test.

T1 differences (ΔT1) were compared between the groups at each time point using two-tailed unpaired t-tests. A negative ΔT1 was considered as no passage. A two-way ANOVA (mixed effects) was used to analyse differences between the groups over time. Tukey's multiple comparisons test was used to perform post-hoc comparisons.

Brain metabolite levels of Glx, mI, NAA and total choline (tCho) in the ACC and insula were analysed with a two-way ANOVA (mixed effects) using the Geisser-Greenhouse correction. Post-hoc comparisons were performed using the Tukey's multiple comparisons test.

Passage of FD4 and TRITC-70 after 3 hours (representing small intestinal permeability) and after 24 hours (representing colonic intestinal permeability) was analysed with a two-way-ANOVA (mixed effects) using the Geisser-Greenhouse correction. Post hoc comparisons were performed using Tukey's multiple comparisons test. TEER values, potential difference (dP), FD4 and TRITC70 passage from the Ussing experiment were analysed using unpaired t-tests.

Two-way ANOVA (mixed effects) was used to analyse motility and glycaemia levels. Tukey's multiple comparisons test was used for post-hoc analysis.

To assess the relationship between the behavioural, somatic, intestinal and neurological parameters across all time points, a Spearman rank correlation was performed.

Results

Gut permeability and motility analyses *in vivo*.

The paracellular and the transcellular small intestinal permeability were not different between the BBDR and BBDP groups. In contrast, the colonic paracellular permeability was increased in the BBDP group (ANOVA p<0.05, Figure 4A) only at day 90. In contrast, the colonic transcellular permeability was overall strongly increased in the BBDP group (Figure 4B, ANOVA p<0.0001) at 30, 90, and 160 days.

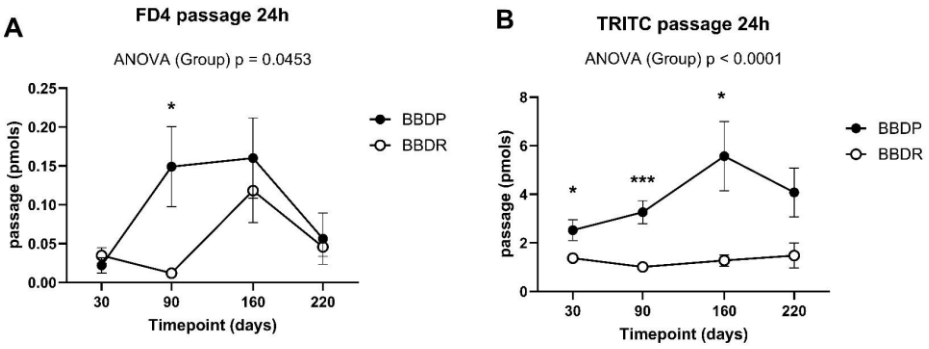

Figure 4 – In vivo passage of FD4 (A) and TRITC70 (B) in the colon
This figure *represents paracellular and transcellular passage, respectively, after 24 hours for BBDP and BBDR rats at day 30, 90, 160 and 220 is shown. The BBDP group had an increased passage of FD4 at day 90 and of TRITC70 at day 30, 90 and 160 compared to the BBDR group. *p<0.05, ***p<0.001. BBDP (N=6-14) and BBDR (N=11-16). Data are expressed as mean ± SEM.*

BBDP rats had a reduced GI transit time (ANOVA p=0.003, Figure 5) at day 90 (664.2 vs. 495.7 min, p=0.001), but not at the other time points.

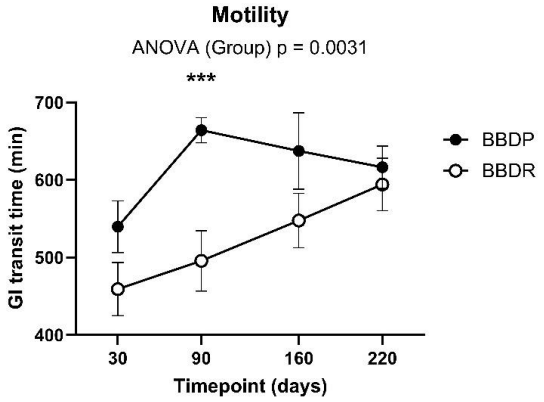

Figure 4 - Gastrointestinal transit time of BBDP and BBDR rats

*This is shown at day 30, 90, 160 and 220. BBDP rats had a significantly slower transit time compared to BBDR rats. ***p<0.001. BBDP (N=6-14) and BBDR (N=11-16) rats. Data are expressed as mean ± SEM.*

Gut permeability analyses *ex vivo* in Ussing Chambers

At 220 days, the transepithelial electrical resistance (TEER, 39.45 vs. 42.53 Ω x cm², p=0.5), potential difference (dP) and the paracellular FD4 passage (18.77 vs. 19.89 pmols, p=0.8), and the transcellular TRITC70 passage (0.1 vs. 0.058 pmols, p=0.3) did not differ between groups (Figure 6).

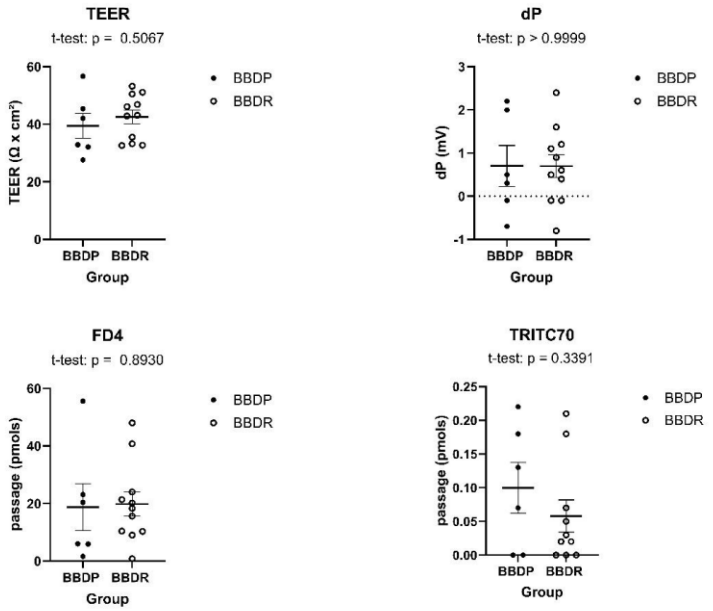

Figure 5 - Ex vivo permeability assessed by Ussing chamber

It revealed no differences in TEER, potential difference (dP), FD4 passage and TRITC70 passage between BBDP and BBDR rats. BBDP N=6 and BBDR N=11 rats. Data are expressed as mean ± SEM.

Blood-brain barrier (BBB) integrity analysis *in vivo.*

The BBB permeability in the BBDP was slightly increased in the ACC at later time points (160 and 220 days, figure 7), while the hippocampus and the insula (Figure 8) remained unaffected.

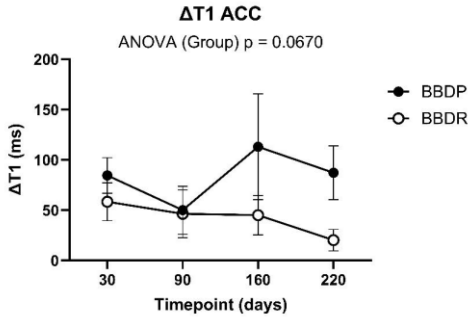

Figure 6 - Longitudinal ΔT1 values are shown for the ACC *for each group at day 30, 90, 160 and 220. No significant differences were seen between the groups and over time. Data are expressed as mean ± SEM.*

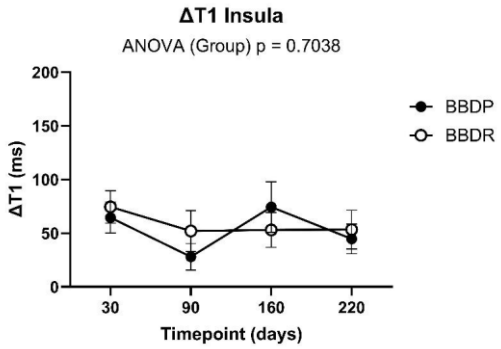

Figure 7 - Longitudinal ΔT1 values are shown for the insula *for each group at day 30, 90, 160 and 220. No significant differences were seen between the groups and over time. Data are expressed as mean ± SEM.*

Brain metabolites analysis (neuroinflammation) in the ACC and insula *in vivo*.

BBDP rats did not show signs of neuroinflammation in the ACC or the insula, as myoinositol and total Choline levels were not altered (Figures 9B and 10B). BBDP rats also have higher concentrations of glutamine plus glutamate (Glx, Figure 9A) in the insula.

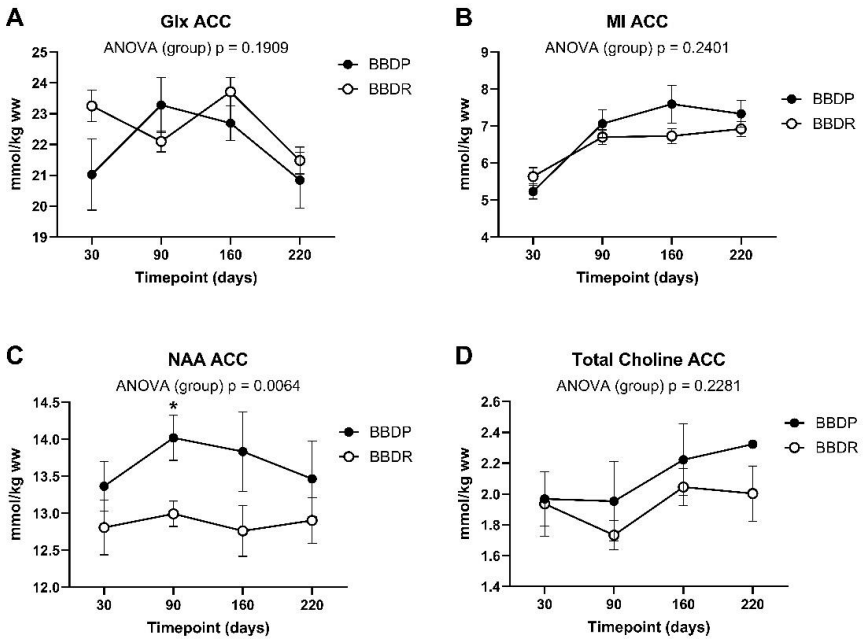

Figure 8 - Concentrations of Glx, MI, NAA, and total choline*(in mmol/kg wet weight) in the ACC in the BBDP and BBDR rats at day 30, 90, 160, and 220. BBDP rats had higher levels of NAA. Both groups had increasing levels of MI over time. *p<0.05. Data are expressed as mean ± SEM in BBDP (N=6-13) and BBDR: (N=10-16).*

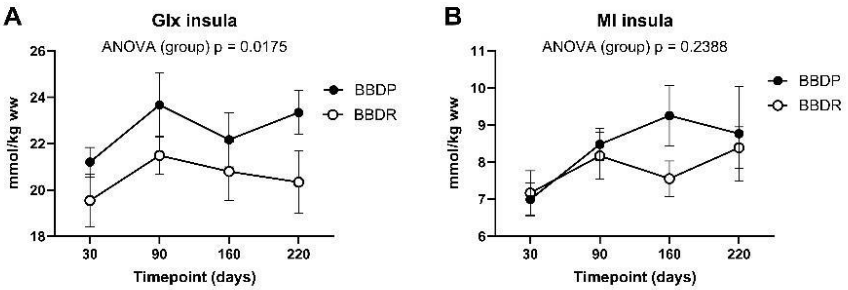

Figure 9 - Concentrations of Glx and MI(in mmol/kg wet weight) in the insula *of the BBDP and BBDR rats at day 30, 90, 160, and 220. BBDP rats had higher levels of Glx. Data are expressed as mean ± SEM in BBDP (N=6-13) and BBDR: (N=10-16).*

Nociception/pain (the tail-flick test) analysis.

Although there was no overall significant difference in tail-flick latency time between the BBDP and BBDR groups (ANOVA p=0.09, Figure 11), the posthoc comparisons revealed a significantly shorter latency time in the BBDP group (1.435 vs. 1.768 s, p=0.01) at day 30.

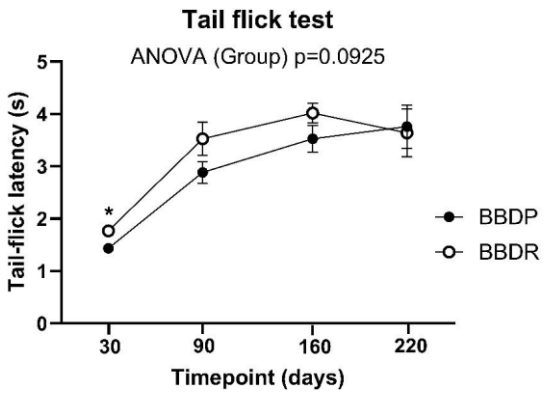

Figure 10 - Somatic pain sensitivity in the BBDP and BBDR rats *at day 30, 90, 160 and 220 assessed by the tail flick test. The figure shows the average latency time of three measures. BBDP rats (N=9-15) and BBDR rats (N=13-16). *p<0.05. Data is expressed as means ± SEM.*

Behavioural assessment of anxiety (the elevated plus maze).

The number of open entries in the open arms was significantly higher in BBDP rats (ANOVA p=0.0020) compared to BBDR control rats at day 30 (7.3 vs. 3.8 entries, p=0.0017) and day 90 (6.4 vs. 3.5 entries, p=0.0023) but not at day 160 and 220 (p>0.05) (Figure 12A).

BBDP rats spent more time in the open arms (ANOVA p<0.0001) at day 30 (34.22 vs. 12.08 s, p=0.0002) and 90 (24.42 vs. 11.51 s, p=0.01) but not at days 160 and 220 (p>0.05) (Figure 12B).

A

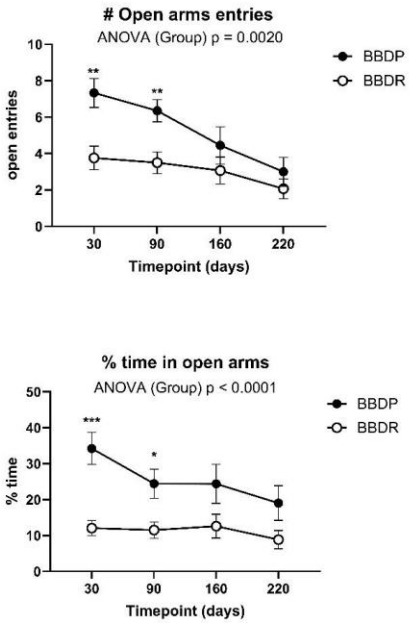

Figure 11 - Decreased anxiety-like behaviour *was seen in BBDP rats compared to BBDR rats in the elevated plus maze test. The figure shows open arm entries (A), and percentage of time spent in the open (B) arms. BBDP rats (N=10-15) and BBDR rats (N=14-17). *p<0.05, **p<0.01, ***p<0.001, ****p<0.0001. Data are expressed as means ± SEM.*

Association of intestinal permeability and brain parameters.

Colonic passage of TRITC70 was significantly correlated with BBB permeability in the ACC (ρ=0.40, p=0.002) but not with the concentration of metabolites in the ACC and the insula. This finding indicates that colonic transcellular permeability could drive only some of the brain alterations.

Conclusion

Despite the longitudinal nature of the study in the BBDP rat model, it is difficult to quickly establish a cause-relationship and the link between increased colonic permeability and brain dysfunction, and consequently comorbidities such as anxiety and altered somatic nociception. However, our findings in the BBDP rats show that an altered BBB is only present in specific brain regions, and signs of brain neuroinflammation are not present in this IBS preclinical rat model. These findings and the human data of D4.1 in IBS patients

will be further evaluated and completed by taking into account the data analysis of the other two rat models.

Author contributions: The DISCOvERIE consortium produced this report. Data was collected in two centers: UCC and KUL. WP4 co-leader Prof. Ricard Farre and his staff (Alice Rustichelli) gathered the information from the contributing centers, performed the analyses, and wrote the report.

References

1 Drossman, D. A. Functional Gastrointestinal Disorders: History, Pathophysiology, Clinical Features and Rome IV. *Gastroenterology*, doi:10.1053/j.gastro.2016.02.032 (2016).

2 Oka, P. *et al.* Global prevalence of irritable bowel syndrome according to Rome III or IV criteria: a systematic review and meta-analysis. *Lancet Gastroenterol Hepatol* **5**, 908-917, doi:10.1016/S2468-1253(20)30217-X (2020).

3 Petersen, M. W. *et al.* Irritable bowel, chronic widespread pain, chronic fatigue and related syndromes are prevalent and highly overlapping in the general population: DanFunD. *Sci Rep* **10**, 3273, doi:10.1038/s41598-020-60318-6 (2020).

4 Zamani, M., Alizadeh-Tabari, S. & Zamani, V. Systematic review with meta-analysis: the prevalence of anxiety and depression in patients with irritable bowel syndrome. *Aliment Pharmacol Ther* **50**, 132-143, doi:10.1111/apt.15325 (2019).

5 Woting, A. & Blaut, M. Small Intestinal Permeability and Gut-Transit Time Determined with Low and High Molecular Weight Fluorescein Isothiocyanate-Dextrans in C3H Mice. *Nutrients* **10**, doi:10.3390/nu10060685 (2018).

6 Gonzalez-Gonzalez, M. *et al.* Investigating Gut Permeability in Animal Models of Disease. *Front Physiol* **9**, 1962, doi:10.3389/fphys.2018.01962 (2018).

7 Thomson, A. *et al.* The Ussing chamber system for measuring intestinal permeability in health and disease. *BMC Gastroenterol* **19**, 98, doi:10.1186/s12876-019-1002-4 (2019).

8 Westerhout, J., Wortelboer, H. & Verhoeckx, K. in *The Impact of Food Bioactives on Health: in vitro and ex vivo models* (eds K. Verhoeckx *et al.*) 263-273 (2015).

9 Hole K, T. A. *Encyclopedia of Pain*. (Springer Berlin Heidelberg, 2013).

10 Walf, A. A. & Frye, C. A. The use of the elevated plus maze as an assay of anxiety-related behavior in rodents. *Nat Protoc* **2**, 322-328, doi:10.1038/nprot.2007.44 (2007).

11 Lezak, K. R., Missig, G. & Carlezon, W. A., Jr. Behavioral methods to study anxiety in rodents. *Dialogues Clin Neurosci* **19**, 181-191, doi:10.31887/DCNS.2017.19.2/wcarlezon (2017).

12 Lohrke, J. *et al.* 25 Years of Contrast-Enhanced MRI: Developments, Current Challenges and Future Perspectives. *Adv Ther* **33**, 1-28, doi:10.1007/s12325-015-0275-4 (2016).

13 Donatelli, G. *et al.* Quantitative T1 mapping detects blood-brain barrier breakdown in apparently non-enhancing multiple sclerosis lesions. *Neuroimage Clin* **40**, 103509, doi:10.1016/j.nicl.2023.103509 (2023).

14 Paxinos G, W. C. *The Rat Brain in Stereotaxic Coordinates*. 7th edn, 480 (2013).

15 Buonocore, M. H. & Maddock, R. J. Magnetic resonance spectroscopy of the brain: a review of physical principles and technical methods. *Rev Neurosci* **26**, 609-632, doi:10.1515/revneuro-2015-0010 (2015).

16 Jansen, J. F., Backes, W. H., Nicolay, K. & Kooi, M. E. 1H MR spectroscopy of the brain: absolute quantification of metabolites. *Radiology* **240**, 318-332, doi:10.1148/radiol.2402050314 (2006).

17 Oberg, J. *et al.* Age related changes in brain metabolites observed by 1H MRS in APP/PS1 mice. *Neurobiol Aging* **29**, 1423-1433, doi:10.1016/j.neurobiolaging.2007.03.002 (2008).

18 Provencher, S. W. Estimation of metabolite concentrations from localized in vivo proton NMR spectra. *Magn Reson Med* **30**, 672-679, doi:10.1002/mrm.1910300604 (1993).

19 Provencher, S. W. Automatic quantitation of localized in vivo 1H spectra with LCModel. *NMR Biomed* **14**, 260-264, doi:10.1002/nbm.698 (2001).

20 Glover, G. H. Overview of functional magnetic resonance imaging. *Neurosurg Clin N Am* **22**, 133-139, vii, doi:10.1016/j.nec.2010.11.001 (2011).